

Phase transformation kinetics in polycrystalline $\text{Fe}_x\text{Al}_{1-x}$ ($x \geq 0.6$) alloys: Experiment and Simulation

Artem A. Nazarov^{1,2}, Igor Y. Pashenkin¹, Dmitry A. Tatarskiy^{1,2}, Pavel A. Yunin^{1,2}, Sergey A. Churin¹, Maksim V. Sapozhnikov^{1,2}, Andrey A. Fraerman¹, Murtaza Bohra³, Nikolay I. Polushkin¹

¹*Institute for Physics of Microstructures, Russian Academy of Sciences,
Akademicheskaya St. 7, 603087, Nizhny Novgorod, Russia*

²*Lobachevsky State University, Nizhny Novgorod 603950, Russia*

³*Mahindra University, Hyderabad, 380 Telangana 500043, India*

The presence of defects of different kinds, e.g., vacancies, voids, dislocations, grain boundaries, and surfaces, in realistic materials can strongly modify and even dictate the thermodynamics of phase transformations. Our study demonstrates, both theoretically and experimentally, that in the ordering of $\text{Fe}_x\text{Al}_{1-x}$ ($x \geq 0.6$) alloys subjected to high-temperature treatment, the relaxation of the as-prepared chemically disordered alloy into the ordered B2 state is hampered by another process. A manifestation of this is an increase in the alloy's magnetization. A plausible explanation for a nonmonotonous behavior of the magnetization we observe is segregation of Al into structural defects, e.g., grain boundaries, and thus purification of the Fe host lattice. Qualitatively, experimental findings reported here are supported by molecular dynamics simulation of the phase transformation kinetics in $\text{Fe}_x\text{Al}_{1-x}$. These studies can be useful for choosing the preparation strategy for functional alloys.

1. Introduction

The thermodynamics and kinetics of phase transitions has been a steady research arena in condensed matter and materials physics through decades [1, 2]. Most of the existing theoretical studies of phase transitions have focused on nearly defect-free bulk crystals, which is often sufficient to capture the general thermodynamic trends. However, in most cases intrinsic and extrinsic defects are present in materials, and they may alter the thermodynamics and kinetics of phase transitions [3, 4]. One of interesting manifestation of the defect-depended phase transition kinetics is surface segregation of one of the alloy components [4-7]. More commonly, it is energetically profitable to impurities to migrate to structural defects like grain boundaries, dislocations or free surfaces, thus purifying the host matrix. The processes of such a kind were observed experimentally in phase-separating alloys like Ni-Cr [5, 6] and Ni-Cu [7] having the broad miscibility gaps in their phase diagrams.

Here, we report evidences of surface segregation in alloys with opposite trend in their relaxation to the phase equilibrium, which is chemical ordering in the atomic lattice. In ordering alloys, activation of such a process is less expected [8]. In our attempts to chemically order thin

films of $\text{Fe}_x\text{Al}_{1-x}$ ($x \geq 0.6$) alloy by aging them at elevated temperatures T , we find the non-monotonic behavior of film magnetization. If the magnetization decreases at sufficiently low T , which reflects chemical ordering in the system [9-12], it starts to increase with increasing T . The magnetization enhancement we observe is associated with segregation of Al into various defects occurring in the lattice, e.g., vacancies, voids, grain boundaries, film surface, etc. Importantly, our experimental observations are supported by molecular dynamics (MD) simulations of aging in $\text{Fe}_x\text{Al}_{1-x}$. These simulations were performed by comparing the kinetics of phase transformation in polycrystalline alloys and a single (defect-free) crystal.

2. Materials and Methods

Sample preparation. Fe_xAl_x films were prepared with a thickness of 50 nm using dc magnetron co-sputtering from individual Fe and Al targets onto Si (100) substrates with a native SiO_2 surface layer. In these experiments, an AJA 2200 multichamber system was used at a basic pressure down to $\sim 6 \times 10^{-8}$ mbar. The film composition was checked by measuring the critical angle for X-ray total reflection using a Bruker D8 Discover x-ray diffractometer. The as-grown samples were aged at elevated T ranging from 300°C to 900°C. The heat treatments were performed in a rapid thermal annealing (RTA) system operated with He gas flowing through a heated sample at a flow rate of 10 l/min and a pressure of 1.5 kg/cm².

Sample characterization. The phase transformations occurring in the films under RTA aging were studied with selected area electron diffraction (SAED) in the transmission electron microscopy (TEM) mode and magneto-optical Kerr effect (MOKE) magnetometry. Taking TEM micrographs and SAED data from the samples prepared on commercial 50 nm thick Si_3N_4 membranes allowed for determining the averaged grain diameter (10.5 ± 1.0 nm in the as-grown films) in the polycrystalline structure and the long-range order S , respectively [13, 14]. The degree of chemical order was estimated as [15]

$$S = \sqrt{(I_{100}/I_{110})_{\text{exp}}} / \sqrt{(I_{100}/I_{110})_{\text{theor}}} , \quad (1)$$

where $(I_{100}/I_{110})_{\text{exp(theor)}}$ are ratios between intensities of 100 superstructure (B2 structure) and 110 fundamental diffraction peaks, which are found experimentally and by calculations in the ideal B2 structure. The used MOKE setup was home-built and based on a Faraday modulator technique. As a light source, a He-Ne laser ($\lambda=633$ nm, 5 mW, Thorlabs HRS015B) was employed. The MOKE intensity was measured at *room temperature* as a function of magnetic field H applied in the film plane to generate a MOKE hysteresis loop. The accuracy of measuring the Kerr rotation angle θ in this MOKE setup was ~ 0.1 mrad.

Simulations. MD simulations have been performed by aging of the supercell in $\text{Fe}_{0.6}\text{Al}_{0.4}$ at elevated temperatures by using resources of the Lobachevsky Supercomputer Center. Two types of a chemically disordered $\text{Fe}_{0.6}\text{Al}_{0.4}$ state, namely a polycrystal and single crystal, were studied by using the ATOMSK software [16] with the cif-file (607483-ICSD) for the Im-3m A2 phase in $\text{Fe}_{0.6}\text{Al}_{0.4}$. The monocrystal was obtained by multiplying the supercell along three directions to have dimensions of $5 \times 5 \times 5 \text{ nm}^3$ and to consist of $\sim 10^4$ atoms. To build a polycrystal, the Voronoi diagram method was used upon the basis of the ATOMSK software. The polycrystal had dimensions of $15 \times 15 \times 15 \text{ nm}^3$ (~ 260000 atoms) and consisted of several grains with diameters in a few nanometers. The alloy composition chosen ($x=0.6$) was set by random substitution of a fraction of Al atoms by Fe ones. The simulation used periodic boundary conditions in all three directions. To describe the interatomic interaction of Al-Fe, the EAM (Embedded-Atom Method) potential was used [17]. Upon completion of annealing, the supercell slowly cooled to room temperature. Visualization of the calculated structures was carried out using the OVITO software package [18].

3. Results and Discussion

Experiment. In our experiments we find that the samples with different concentrations of Al in the binary $\text{Fe}_x\text{Al}_{1-x}$ system behave in a different manner with increasing T . Figure 1 (a) shows the MOKE responses $2\theta_s$ of two polycrystalline $\text{Fe}_x\text{Al}_{1-x}$ films as a function of T . In one of them $x=0.6$, whereas $x=0.7$ in the other one. At each T , a MOKE response shown in Figure 1 is close to its asymptotic value achievable under RTA aging [14]. Values of θ_s presented are Kerr rotation angles in an applied magnetic field which saturates film magnetization.

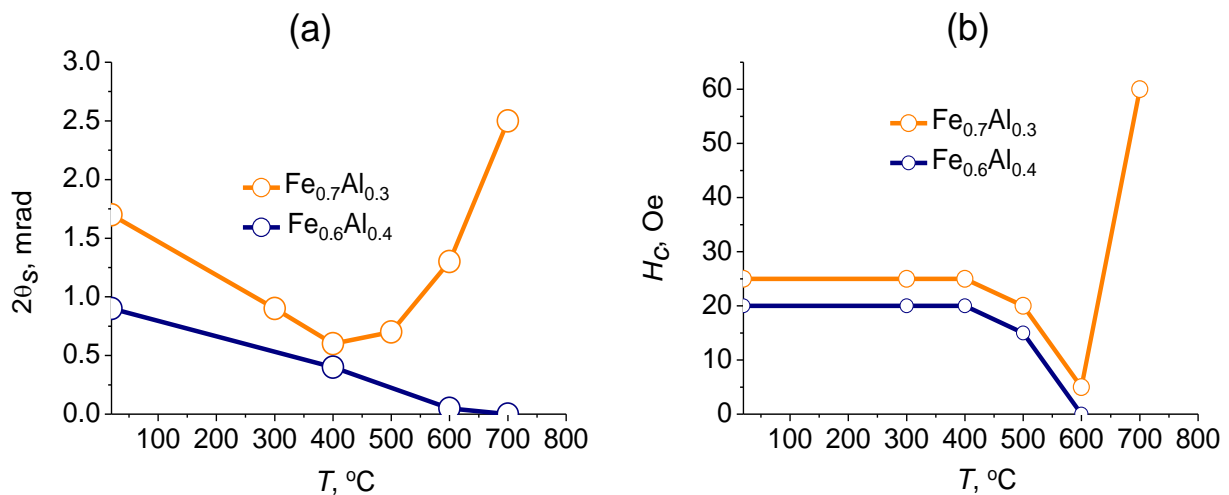


Figure 1: MOKE response $2\theta_s$ (a) and coercivity H_c (b) in polycrystalline $\text{Fe}_x\text{Al}_{1-x}$ films at $x=0.6$ and $x=0.7$ as a function of annealing temperature T .

We see that magnetization in $\text{Fe}_{0.7}\text{Al}_{0.3}$ behaves nonmonotonously with increasing aging temperature to $T=700$ °C. At sufficiently low $T<400$ °C, it decreases, which is similar to the behavior of $\text{Fe}_{0.6}\text{Al}_{0.4}$ and can reflect chemical ordering in the alloy [9-12]. However, at $T\geq 500$ °C, magnetization in $\text{Fe}_{0.7}\text{Al}_{0.3}$ increases, which could rather signify the start of the disordering process. In addition, we show how the coercivity H_c in $\text{Fe}_{0.7}\text{Al}_{0.3}$ behaves with annealing temperature. As there is only a slight enhancement of H_c at $T\geq 500$ °C, which corresponds to the increase in film magnetization, it is likely that the magnetic structure remains still homogeneous in the film. Such a temperature behavior evidences purification of Fe in the $\text{Fe}_x\text{Al}_{1-x}$ atomic lattice due to Al segregation into structural defects, e.g., grain boundaries, in our polycrystalline films. Obviously, Al segregation can hamper the ordering process what we observe.

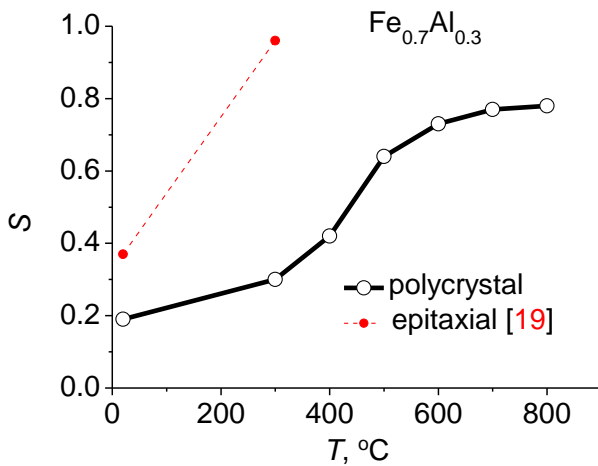


Figure 2: S versus T in polycrystalline $\text{Fe}_{0.7}\text{Al}_{0.3}$ films. For comparison, values of S obtained in epitaxial $\text{Fe}_{0.7}\text{Al}_{0.3}$ films [19] are also shown.

Figure 2 shows the S -versus- T dependence in our polycrystalline $\text{Fe}_{0.7}\text{Al}_{0.3}$ samples. We find that the retardation of the ordering process occurs at $T>500$ °C. For comparison, we show the literature data on values of S , which were obtained in thin-film $\text{Fe}_{0.7}\text{Al}_{0.3}$ samples grown on MgAl_2O_4 (001) single crystal substrates by molecular beam epitaxy at room temperature and its elevation. It was found in Ref. [19] that the nearly ideal B2 structure ($S=0.96$) forms in the epitaxial films of $\text{Fe}_{0.7}\text{Al}_{0.3}$ grown at 300 °C.

Modeling. Figure 3 shows atomic structures in the $\text{Fe}_{0.6}\text{Al}_{0.4}$ single crystal, which have been simulated at $T=1100$ °C for different times of aging, 10 ns, 40 ns, and 60 ns. As seen, at least partial ordering in the atomic lattice occurs at such timescale and aging temperature. To quantify this ordering process, we computed the ordering degree S using Equation (1). Table 1 gives this quantity its temporal dependence for both a single crystal and polycrystal. In this evaluation, we assumed that $(I_{100}/I_{110})_{\text{theor}} = 0.8 \times 0.19$ [20] in the B2- $\text{Fe}_{0.6}\text{Al}_{0.4}$ structure, in which all Al atoms occupy positions in the Al sublattice.

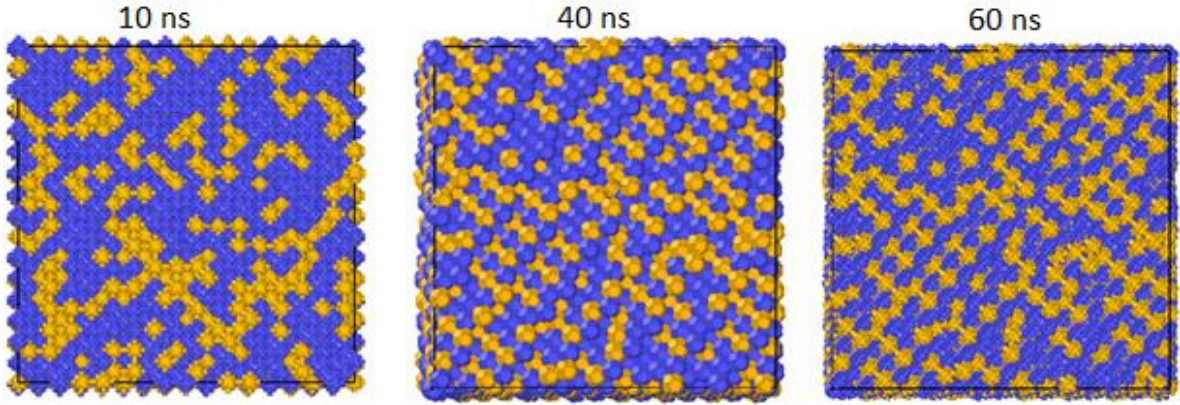


Figure 3: Visualization of the atomic structure in a $\text{Fe}_{0.6}\text{Al}_{0.4}$ single crystal simulated for different aging times at $T=1100$ °C. Blue and yellow tones are Fe and Al atoms, respectively.

Table 1. Ordering degree S for mono- and polycrystalline $\text{Fe}_{0.6}\text{Al}_{0.4}$ at different aging times. This quantity was calculated from the atomic structures shown in Figure 3.

Object type	Ordering degree S		
	10 ns	40 ns	60 ns
Monocrystal	0.11	0.32	0.46
Polycrystal	0.026	0.031	0.035

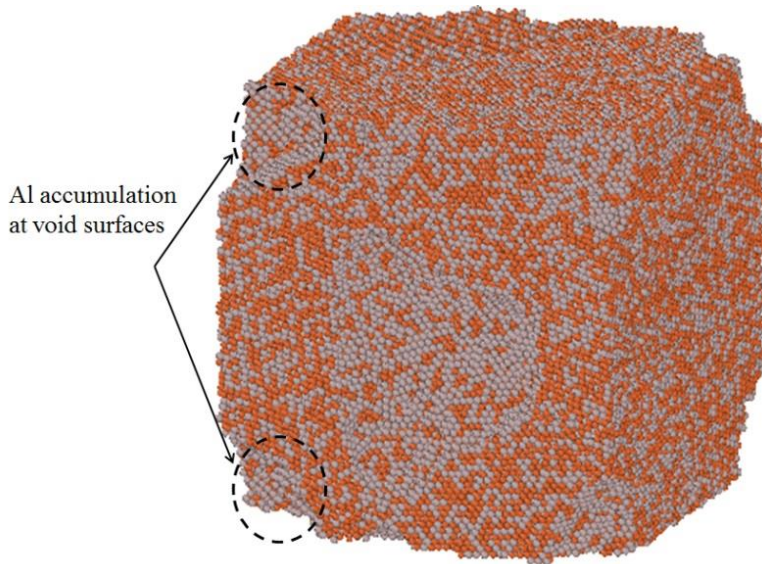


Figure 4: Visualization of Al segregation in the $\text{Fe}_{0.6}\text{Al}_{0.4}$ polycrystal with embedded voids. The process was activated for 20 ns at 1100 °C.

Table 1 highlights a difference in ordering rates between a mono- and poly-crystal. We see a significant reduction of the ordering rate in the polycrystal. This is compatible with the experimental data presented in Figure 2. However, it is hard to visualize Al segregation into grain boundaries because of a strong enlargement of crystalline grains under aging at high T . Therefore, we have studied the phase

transformations in a polycrystal with embedded voids. Figure 4 shows such a system, where gray and red tones are Al and Fe atoms. We see segregation and accumulation of Al atoms at internal surfaces of the voids.

4. Conclusions

The kinetics of ordering in thin (50 nm) films of $\text{Fe}_x\text{Al}_{1-x}$ ($x \geq 0.6$) alloys was studied experimentally. It is found that magnetization in polycrystalline $\text{Fe}_x\text{Al}_{1-x}$ behaves nonmonotonously with elevation of annealing temperature (at least, if $x=0.7$). This feature evidences Al segregation into structural defects such as grain boundaries. Comparison of our data on polycrystalline films of $\text{Fe}_x\text{Al}_{1-x}$ to the literature data on epitaxial films with the same composition supports the conclusion about Al segregation. Finally, we find that the kinetics of phase transformations in $\text{Fe}_x\text{Al}_{1-x}$ observed experimentally is consistent with the results of simulations performed with the molecular dynamics method.

Acknowledgements

Work was supported by the Russian Science Foundation (grant no. 23-22-00044).

References

1. J. Ortin, Thermodynamics and Kinetics of Phase Transitions. In: Berveiller, M., Fischer, F.D. (eds) Mechanics of Solids with Phase Changes. International Centre for Mechanical Sciences, vol 368. (Springer, Vienna, 1997); https://doi.org/10.1007/978-3-7091-2660-8_1.
2. D. Lencer, M. Salinga, B. Grabowski, T. Hickel, J. Neugebauer, and M. Wuttig, A map for phase-change materials, *Nat. Mater.* **2008**, 7, 972-977.
3. S. Korte-Kerzel, T. Hickel, L. Huber, D. Raabe, S. Sandlöbes-Haut, M. Todorova, and J. Neugebauer, Defect phases – thermodynamics and impact on material properties, *Int. Mater. Rev.* **2022**, 67 (1), 89-117.
4. X. Zhang, J. Zhang, H. Wang, J. Rogal, H.-Y. Li, S.-H. Wei, T. Hickel, Defect-characterized phase transition kinetics. *Appl. Phys. Rev.* **2022**, 9 (4), 041311.
5. M. Bohra, P. Grammatikopoulos, R. E. Diaz, V. Singh, J. Zhao, J.-F. Bobo, A. Kuronen, F. Djurabekova, K. Nordlund, and M. Sowwan, Surface Segregation in Chromium-Doped NiCr Alloy Nanoparticles and Its Effect on Their Magnetic Behavior, *Chem. Mater.* **2015**, 27 (9), 3216–3225.
6. V. Alman, A. Annadi, M. Bohra, C. Murapaka, J. Pradhan, A. Haldar, and V. Singh, Thickness-Driven Magnetic Behavior in Ni–Cr Nanocrystalline Thin 2 Films: Implications for Spintronics and Magnetic Cooling, *ACS Applied Nano Materials* **2023** 6 (12), 10394-1041.
7. V. Leontyev, Magnetic properties of Ni and Ni-Cu nanoparticles, *Phys. Status Solidi B* **2013**, 250 (1), 103–107.
8. M. Polak, L. Rubinovich, The interplay of surface segregation and atomic order in alloys, *Surface Science Reports* **2000**, 38, 127-194.
9. J. Ehrler, B. Sanyal, J. Grenzer, S. Zhou, R. Böttger, B. Eggert, H. Wende, J. Lindner, J. Fassbender, C. Leyens, K. Potzger, and R. Bali, Magneto-structural correlations in a systematically disordered B2 lattice, *New J. Phys.* **2020**, 22, 073004.
10. J. Kudrnovský, V. Drchal, and F. Máca, I. Turek, S. Khmelevskyi, Large anomalous Hall angle in the $\text{Fe}_{60}\text{Al}_{40}$ alloy induced by substitutional atomic disorder, *Phys. Rev. B* **2020**, 101, 054437.
11. N. I. Polushkin, T. B. Möller, S. A. Bunyaev, A. V. Bondarenko, M. He, M. V. Shugaev, J. Boneberg, and G. N. Kakazei, Simulation of chemical order–disorder transitions induced thermally at the nanoscale for magnetic recording and data storage, *ACS Appl. Nano Mater.* **2020**, 3 (8), 7668-7677.

12. K. Toyoki, D. Kitaguchi, Y. Shiratsuchi, R. Nakatani, Influence of long- and short-range chemical order on spontaneous magnetization in single-crystalline $\text{Fe}_{0.6}\text{Al}_{0.4}$ compound thin films, *J. Phys.: Condens. Matter* **2024**, *36*, 135805.
13. I. Y. Pashenkin, R. V. Gorev, M. A. Kuznetsov, D. A. Tatarskiy, S. A. Churin, P. A. Yunin, M. N. Drozdov, D. O. Krivulin, M. V. Sapozhnikov, E. S. Demidov, V. A. Skuratov, E. V. Kudyukov, G. V. Kurlyandskaya, A. A. Fraerman, and N. I. Polushkin, Magnetic and magnetocaloric modifications near room temperature in $\text{Fe}_{0.6}\text{Al}_{0.4}$ nanoalloys under irradiation by swift heavy ions, *J. Phys. Chem. C* **2024**, *128* (21), 8853–8860.
14. I. Yu. Pashenkin, D. A. Tatarskiy, S. A. Churin, A. N. Nechay, M. N. Drozdov, M. V. Sapozhnikov, N. I. Polushkin, Magneto-optical control of ordering kinetics and vacancy behavior in Fe-Al thin films quenched by laser, <https://www.arxiv.org/abs/2407.16423>.
15. B. D. Cullity, Elements of X-ray Diffraction (Addison-Wesley, Reading, MA, USA, 1956).
16. P. Hirel, AtomsK: A tool for manipulating and converting atomic data files, *Comput. Phys. Commun.* **2015**, *197*, 212-219.
17. M.I. Mendeleev, D.J. Srolovitz, G.J. Ackland, S. Han, Effect of Fe Segregation on the Migration of a Non-Symmetric $\Sigma 5$ Tilt Grain Boundary in Al, *J. Mater. Res.* **2011**, *20*, 208-218.
18. A. Stukowski, Visualization and analysis of atomistic simulation data with OVITO—the Open Visualization Tool, *Modell. Simul. Mater. Sci. Eng.* **2010**, *18*, 015012.
19. B. Lv, P. Liu, Y. Wang, C. Gao, M. S, A large anomalous Hall conductivity induced by Weyl nodal lines in $\text{Fe}_{70}\text{Al}_{30}$. *Appl. Phys. Lett.* **2022**, *121* (7), 072405.
20. <https://www.icdd.com/>; pdf entry #01-078-3470.